buildings

MDPI

Article

System Optimization and Operating Strategy of Single-Stage Air Source Heat Pump with Thermal Storage to Reduce Wind Power Curtailment

Qianyue Ren [1], Chuang Gao [2] and Jie Jia [1,*]

[1] College of Civil Engineering, Taiyuan University of Technology, Taiyuan 030024, China; renqianyue0560@link.tyut.edu.cn
[2] CSSC International Engineering Co., Ltd., Beijing 100121, China; gaochuang@csic602.com.cn
* Correspondence: jiajie@tyut.edu.cn

Abstract: Wind power generation has increased in China to achieve the target of decreasing CO_2 emissions by 2050, but there are high levels of wind curtailment due to the mismatch between electricity supply and demand. This paper proposes a single-stage air source heat pump coupled with thermal storage for building heating purposes. The main objective is to find the proper system designs and operating strategy, which can help to avoid peak demand periods while obtaining minimized running costs and reduced wind energy curtailment. Dynamic simulations were performed using TRNSYS to investigate its use in a typical office building based on an actual electricity tariff, wind power, and meteorological data. The proper system designs, including the tank size and thermal storage temperature, were determined to maximize the system's performance. It was found that a proper combination of the two parameters exists for a specific application. Further, results showed that the use of auxiliary electric heating is necessary for single-stage air source heat pumps to participate in a wind curtailment reduction. The operating strategy of the system was also studied. Results indicate that by implementing a proper operating strategy, non-renewable power consumption can be reduced by 11% for the studied building, with a total wind power utilization of 3348 kWh during the heating season while still satisfying the heating demands of users. These findings can contribute to the green and low-carbon development of the building industry and further enhance the grid's accommodation capacity for renewable energy sources.

Keywords: wind power generation; wind power curtailment; thermal energy storage; space heating; operating strategy; TRNSYS simulation

Citation: Ren, Q.; Gao, C.; Jia, J. System Optimization and Operating Strategy of Single-Stage Air Source Heat Pump with Thermal Storage to Reduce Wind Power Curtailment. *Buildings* **2024**, *14*, 1993. https://doi.org/10.3390/buildings14071993

Academic Editor: Chi Yan Tso

Received: 25 April 2024
Revised: 10 June 2024
Accepted: 14 June 2024
Published: 1 July 2024

1. Introduction

In recent years, wind and photovoltaic power generation has experienced a rapid expansion in China. The increasingly higher proportion of renewable energy integrated into power grids poses a severe challenge due to the random nature of wind and solar powers. Buildings, as major end-users of electricity, can offer "flexible" electricity loads to the grid through the adoption of smart control technology, energy storage, demand response, and other means. Fully leveraging the dispatchable resources on the user side is expected to enhance the grid's capacity to accommodate renewable energy and contribute to the construction of next-generation smart power systems.

In northern China, there is a huge demand for winter heating. Heat pump technology is considered an ideal solution for building heating due to its high operating efficiency. Thermal energy storage (TES), as a demand-side management tool, can also play an important role in avoiding grid overload problems [1]. The combined use of heat pumps and TES offers the possibility to reduce the system's power consumption during peak periods, and part of the electricity demand can be transferred to periods with high renewable energy generation. With this approach, the purpose of load-shifting and reducing wind

curtailment can be achieved simultaneously. Economic benefits are also obtained by taking advantage of the low electricity tariffs in off-peak periods. Existing studies [2–5] have already indicated that the combined use of heat pumps and TES is an effective measure to promote renewable energy utilization, load-shifting, and carbon emission reductions.

In previous studies, cascade heat pumps or CO_2 heat pumps were commonly used as heat source equipment in order to achieve a high heat storage temperature. Khoa et al. [6] proposed a cascade air source heat pump integrated with TES for heat supplies and obtained the optimal operating strategy of the system based on time-of-day tariffs. Wang [7] constructed a coupled CO_2 heat pump and TES heating system. The effects of tank size on the system performance were discussed. Zhang et al. [8] performed a multi-objective optimization on a trans-critical CO_2 heat pump system with TES. The system's performance in terms of its energy, economic, and environmental impact was evaluated. However, these aforementioned works were associated with high initial investments due to the high price of cascade and CO_2 heat pumps. In this respect, a conventional single-stage air source heat pump should be a more suitable option to enhance the system's cost-effectiveness. However, owing to the fact that single-stage air source heat pumps have limited water supply temperatures (around 50 °C), an auxiliary heating means should be incorporated to achieve the desired heat storage temperature.

In previous studies, many researchers have evaluated the impact of various factors on system performance. Jacopo et al. [9] coupled a heat pump with a TES tank for space heating and a domestic hot water supply. The influence of various factors, such as weather conditions, user behavior, and hot water demand, was evaluated. Peter et al. [10] and Maarten et al. [11] studied energy flexibility under different electricity pricing structures, identifying real-time pricing as the most advantageous. Badescu et al. [12] examined the impact of TES tank sizes on system performance. Lyu et al. [13] investigated the influence of air source heat pump capacities on the system's energy-saving potential. However, these studies focused on the impact of different factors on the system, whereas they did not truly conduct the optimization of system operating strategies.

In existing studies, load-shifting was taken as the primary goal for the system's operation. Miaraet al. [14] analyzed system control strategies, TES, and heat pump capacities for twelve scenarios with the goal of load-shifting. Arteconi et al. [15] investigated a heat pump system combined with TES to flatten the grid curve. Kelly et al. [16] investigated the amount of thermal buffering required to shift the operation time of an air source heat pump to off-peak periods. In these studies, the system was evaluated in terms of thermal comfort, energy consumption, and running costs. There is a lack of research that quantifies the system's potential to reduce wind curtailment.

Currently, there are two main control methods to achieve optimal control of the system: non-predictive control and model-based optimal control. While the latter has been found to outperform the former at achieving control goals (e.g., maximizing carbon emissions [17], minimizing operating costs [18,19], or maximizing wind power utilization [20]), it inevitably faces challenges of excessive computation and high costs [21]. In contrast, non-predictive control does not necessitate complex models or extensive data resources, making it simpler to design and operate, but it still maintains good performance and robustness [22]. As a type of non-predictive control, fixed scheduling is simple and implemented easily and is more suitable for use in existing buildings. Therefore, fixed scheduling is selected for load-shifting in this study.

To address the above concerns, this research proposes an integrated heating system based on a single-stage air source heat pump, which has the advantages of low investment costs and easy implementation and is more suitable for the flexible retrofitting of existing systems. In order to raise the storage temperature, an electric heater is used as an auxiliary heating means. The main objective of the study is to investigate the feasibility of the proposed solution in obtaining minimized running costs and reduced wind energy curtailment. Dynamic simulations are performed using TRNSYS to investigate its use in a typical office building based on actual electricity tariffs, wind power, and meteorological

data. The research results can contribute to the green and low-carbon development of the building industry and further enhance the grid's accommodation capacity for renewable energy sources.

2. Materials and Methods

2.1. Basic Data

The northern region of the Beijing–Tianjin–Hebei area is an important wind farm in China. The typical daily wind power generation curve in this region is illustrated in Figure 1. It is evident that wind power exhibits significant fluctuations in a day. Peak wind power generation typically occurs between 2:00 and 8:00, coinciding with the off-peak period of electricity demand. Conversely, the lowest wind power is observed during the early morning, corresponding to the peak period of electricity demand. The above characteristic leads to wind energy dispatch-down, resulting in high levels of wind curtailment. Therefore, the load-shifting control strategies should be designed to operate the system during periods of high wind curtailment, thereby facilitating the increased integration of wind power into the grid.

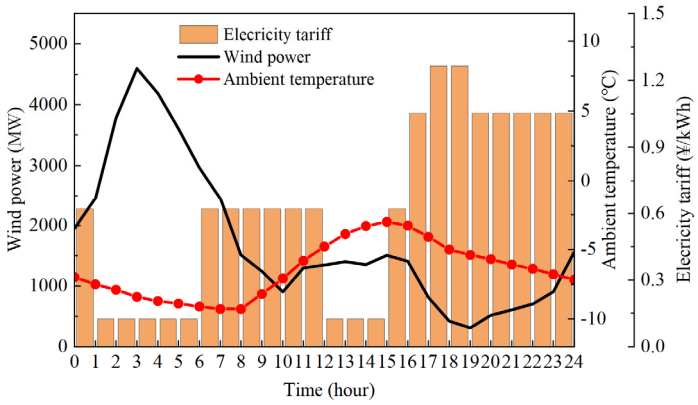

Figure 1. Wind generation, ambient temperature, and electricity tariff in a typical day [23,24].

The operating performance of air source heat pumps is influenced by the ambient temperature. The hourly ambient temperature on a typical day during the heating season in the region is illustrated in Figure 1. It can be observed that the lowest temperatures occur around 8:00, and then the temperatures begin to rise, peaking in the afternoon.

The running costs of the systems are closely related to the electricity tariff adopted. In China, many provinces have implemented time-of-use electricity tariffs to encourage users to adapt their consumption behavior. The electricity tariff adopted in this paper consists of four periods: valley, flat, peak, and sharp peak. In this tariff, the valley rate applies between 01:00–06:00 and 12:00–15:00; the sharp peak rate applies from 17:00 to 19:00.

2.2. Integrated Heating System Configuration

The integrated heating system was comprised of a single-stage air source heat pump coupled with a TES tank. Inside the water tank, electric heaters were installed for auxiliary heating purposes. A schematic of the heating system can be seen in Figure 2.

During the charging period, the air source heat pump was activated to heat the water in the TES tank to 50 °C. Subsequently, the electric heater was employed to elevate the water temperature further to the desired storage temperature set point. Then, there was a lag between the charging and discharging of the stored energy. During the discharging period, the stored high-temperature water was distributed to the fan coil units for space heating. In this period, the activation of the heat pump was switched off, leading to a significant reduction in the system's electricity consumption during peak hours of the grid.

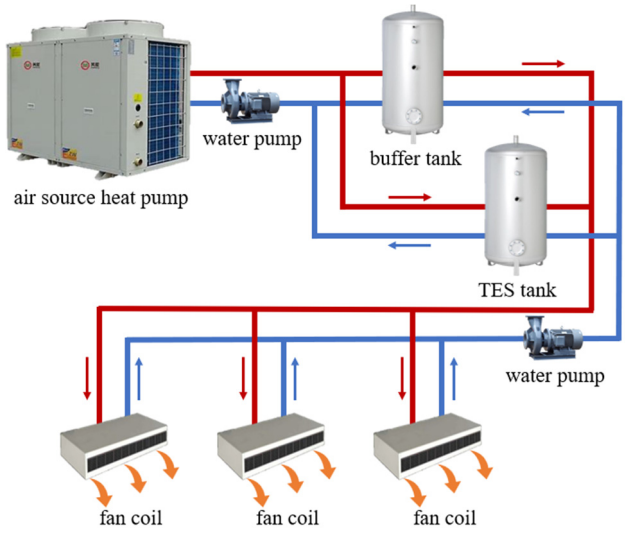

Figure 2. Schematic of the heating system investigated in this study.

2.3. Operating Strategies

This study aimed to seek the proper operation schedule and system design of the air source heat pump coupled with the TES to reduce the grid power demand during peak hours and increase the proportions of wind energy generation while guaranteeing the thermal comfort of the end-user. Therefore, two operating strategies were designed in this paper, taking an office building as the case study. Based on the typical occupants' behaviors, the heating period for the office buildings was set from 9:00 to 19:00. During this period, the heat pump was employed for direct heating from 9:00 to 17:00. From 17:00 to 19:00, the heat pump was deactivated, and heating was provided by the TES tank. Utilizing the TES tank for heating during this period could mitigate the peak load on the power grid and reduce running costs. To ensure normal heating during the day, the TES tank had to be fully charged before 9:00. In this regard, two operating strategies were proposed from the perspective of maximizing wind power utilization and minimizing heat loss of the TES tank. The resulting operating strategies are shown in Figure 3.

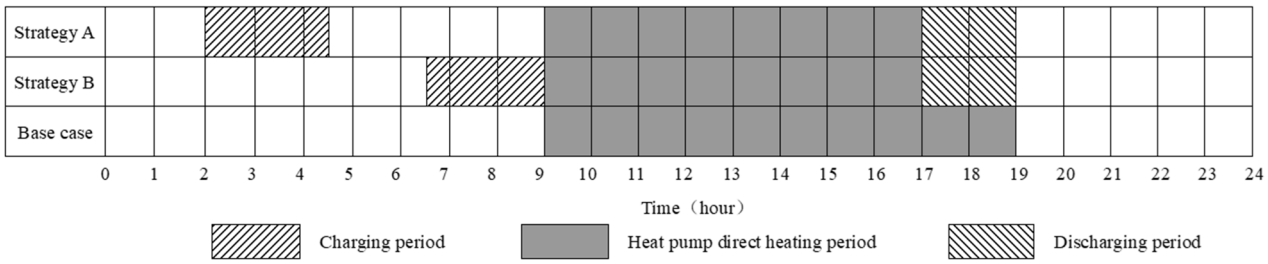

Figure 3. System operating schedules.

2.3.1. Strategy A

In this strategy, the TES tank was charged between 2:00 and 4:30 to take advantage of the peak of wind power generation (Figure 1) while getting the lowest electricity tariff (Figure 1). Then, the stored energy was used during off-peak hours. This operation could help the system maximize the utilization of wind power and reduce running costs.

2.3.2. Strategy B

In this strategy, the tank charging period was assigned to 6:30–9:00 to minimize the heat loss of the tank. There were two reasons for choosing this time period. First, the heat pump needed to be used for direct heating during 9:00–17:00, so the TES tank had to be fully charged before 9:00. Second, a higher capacity of the electric heating was required for

a shorter charging time. Therefore, to maintain the same charging time with Strategy A, the begin time for tank charging was set to 6:30.

2.4. TRNSYS Modeling

To determine the system design parameters such as the water tank size, storage temperature set point, and electric heating power, dynamic simulations of the integrated heating system were conducted using TRNSYS 18 software. The simulation model is illustrated in Figure 4.

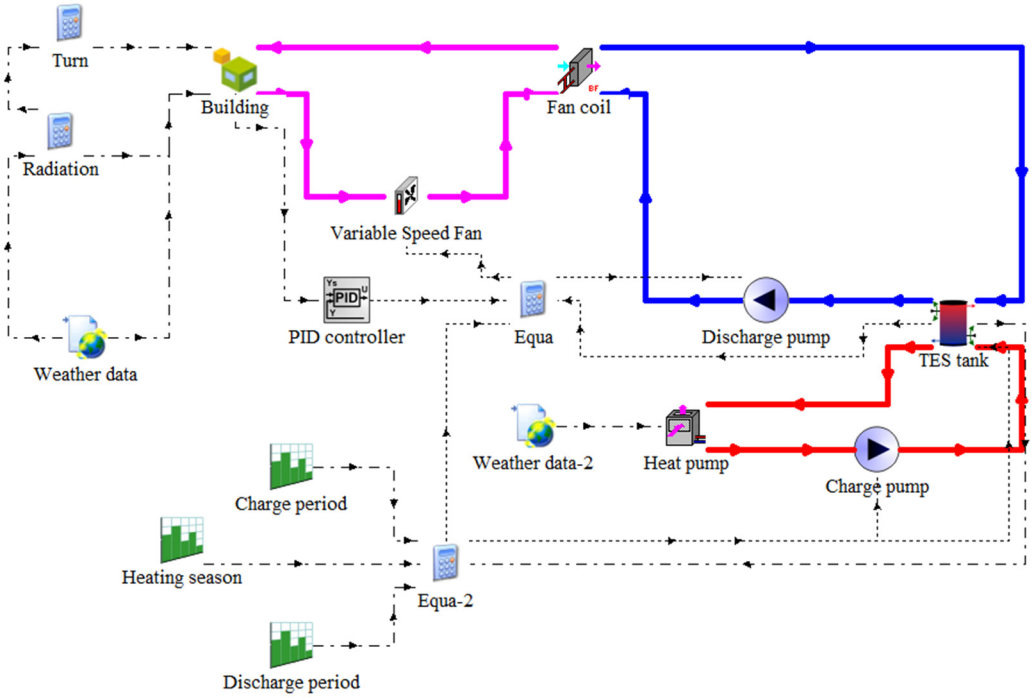

Figure 4. Integrated heating system simulation model.

2.4.1. Target Building

A large open-plan office was selected for detailed simulation studies. The office had external walls on the east, west, and north sides, while the south side was an internal corridor. The ceiling height was 4.2 m, and the total floor area was 486 m^2. There were 12 windows on the north wall, each measuring 2.5 m wide and 1.6 m high. The heat transfer coefficients for the external walls and windows were 0.661 $W/(m^2 \cdot K)$ and 2.36 $W/(m^2 \cdot K)$, respectively. The occupancy density was 6 m^2 per person, with a lighting power density of 9 W/m^2 and an equipment power density of 20 W/m^2. The air infiltration rate was 0.65 times per hour, and the indoor design temperature was set at 20 °C.

2.4.2. Equipment Selection

TRNBUILD 18 was used to model the studied office mentioned above. The peak load occurred at 9:00 on 15th January, reaching 41.5 kW. Based on this peak load, the heat pump selection was made. The chosen heat pump unit was a single-stage fixed-frequency air source heat pump, model MAC-D Plus R22. The real-time performance of the heat pump was simulated using the Type941 module in TRNSYS. The heat pump's heating capacity, power consumption, energy efficiency, and other parameters under different operating conditions could be predicted by this module based on real operating data. The rated parameters of the selected heat pump unit are shown in Table 1. The parameters of other equipment in the system are listed in Table 2.

Table 1. Rated parameters of heat pump unit.

Parameter	Value
Rated heating capacity (kW)	63
Rated Input Power (kW)	16.5
Rated COP	3.82
Rated air volume of evaporator (m^3/h)	22,000
Rated air volume of evaporator (m^3/h)	10.9

Table 2. Other equipment parameters.

Component	Parameter	TRNSYS Type
Thermal storage pump	Rated power = 0.75 kW; Rated flow rate = 10,980 kg/h	Type114
water pump	Rated power = 0.55 kW; Rated flow rate = 3760 kg/h	Type114
PID controller	Proportional coefficient = 4 Integral coefficient = 1.7	Type23
Fan coil unit	Discharge air temperature = 30 °C Rated air flow = 10,200 m^3/h	Type753e

The TES tank was modeled using Type 4c. This module accounted for density variations caused by temperature differences and treated the water in the tank as stratified layers. Energy conservation equations for separate layers were established based on the considerations of the heat exchange between neighboring layers and those with the environment. The energy conservation equation is defined in Equation (1). By discretizing and solving these equations, the distribution of water temperature over different time steps could be obtained. To accurately reflect the temperature field within the tank, ten thermal layers were set in this study. Additionally, by referencing commonly available water tanks in the market, the overall heat loss coefficient per unit area of the tank was set to 2.3 W/(m^2·K). The total heat loss of the tank was calculated according to Equation (2).

The control differential equation for the stratified node i in the tank is as follows:

$$\begin{aligned} m_i C_{fl} \frac{dT_i}{dt} =& \alpha_i m_{heat} C_{fl} (T_{heat} - T_i) + \beta_i m_{load} C_{fl} (T_{load} - T_i) \\ &+ \gamma_i m_{(i-1)} C_{fl} \left(T_{(i-1)} - T_i \right) + \delta_i m_{(i+1)} C_{fl} \left(T_{(i+1)} - T_i \right) \\ &+ \varepsilon \dot{Q}_{aux,i} - U_i \frac{V_i}{H_i} (T_i - T_{env}) \end{aligned} \quad (1)$$

α_i = 1, if fluid from heat source enters node i, 0 otherwise
β_i = 1, if fluid returning from load enters node i, 0 otherwise
γ_i = 1, if the net flow $m_{(i-1)}$ enters node i from the node above
= −1, if the net flow $m_{(i-1)}$ goes from node i to the node above
= 0, if there is no flow stream between node i and the node above
δ_i = 1, if the net flow $m_{(i+1)}$ enters node i from the node below
= −1, if $m_{(i+1)}$ goes from node i to the node below
= 0, if $m_{(i+1)}$ = 0
ε = 1, if auxiliary electric heater is on, 0 otherwise

$$Q_{loss} = \sum_{i=1}^{N} U_i L_t H_i (T_i - T_{env}) + \frac{V_t}{H_t} \left(U_{top} (T_1 - T_{env}) + U_{bot} (T_N - T_{env}) \right) \quad (2)$$

3. Results and Discussion

3.1. Water Tank Size and Storage Temperature Set Point

The amount of thermal energy stored during tank charging is determined by the water tank size and storage temperature set point. If the capacity is set too high, energy consumption for thermal storage will increase. Conversely, if it is set too low, the water temperature during discharging may be too low for space heating, resulting in discomfort for occupants. In this study, a series of simulations were performed to find the proper tank size and temperature set point for the designed load-shifting operating strategies. A total of 36 simulations were run interchangeably with different tank sizes and temperature set points. Three different temperature set points were conducted, including 50 °C, 55 °C, and 60 °C. Additionally, six different tank sizes were considered, ranging from 2.0 m^3 to 3.0 m^3, with an increment of 0.2 m^3. On this basis, the system's performance throughout the heating season (from 15th November to 15th March of the following year) was simulated. The time step for the simulation was set to 0.01 h.

The summary of the simulation results is detailed in Table 3, including the cumulative energy consumption of the system and the total number of hours when the indoor temperature fell below the design temperature (thermal discomfort). Results show a gradual decrease in thermal discomfort hours with an increased storage temperature and water tank size, accompanied by a rise in energy consumption for thermal storage. This was due to the fact that as the temperature set point and the size of the TES tank increased, the amount of thermal energy stored during charging also increased, thereby enhancing the system's ability to offset the heating demand of users and increase the energy consumed for charging purposes.

Table 3. Simulation results for different combinations of tank size and storage temperature.

Storage Temperature Set Point (°C)	Water Tank Size (m^3)	Strategy A		Strategy B	
		Hours of Thermal Discomfort	Thermal Storage Energy Consumption (kWh)	Hours of Thermal Discomfort	Thermal Storage Energy Consumption (kWh)
50	2.00	113	1108.73	91	1178.53
50	2.20	98	1238.94	78	1304.27
50	2.40	90	1366.97	68	1425.43
50	2.60	72	1523.29	54	1533.11
50	2.80	58	1630.47	42	1634.19
50	3.00	49	1724.90	33	1722.13
55	2.00	44	2330.70	32	2435.88
55	2.20	30	2546.44	18	2639.00
55	2.40	19	2789.02	7	2841.17
55	2.60	7	2986.21	2	3023.50
55	2.80	5	3167.49	0	3206.68
55	3.00	0	3352.91	0	3243.54
60	2.00	5	3453.57	2	3486.88
60	2.20	2	3735.23	0	3740.52
60	2.40	0	3995.01	0	3988.44
60	2.60	0	4233.84	0	4215.70
60	2.80	0	4424.49	0	4416.32
60	3.00	0	5013.63	0	5020.79

For Strategy A, the proper storage temperature set point was 55 °C, and the proper tank size was 3 m^3. For Strategy B, 55 °C and 2.8 m^3 were found to be the proper combination of the two parameters. With this system design, Strategy A and Strategy B were able to minimize energy consumption during charging while satisfying the heating demand during the discharging period.

3.2. Auxiliary Electric Heating Power

Once the water tank size and the storage temperature were determined, it was necessary to find a proper heating power for the electric heaters. To this end, extensive simulations were conducted for the two operating strategies. In these simulations, the

heating power ranged from 0 to 13 kW with an increment of 1 kW. Proper heating power was taken as the minimum value of electric heating that could satisfy the heat demand during the discharging period.

The summary of the simulation results is shown in Figure 5. As can be seen, auxiliary electric heating was necessary to ensure the pre-set storage temperature was achieved during tank charging. This was due to the limited supply temperature of the single-stage air source heat pump, and its operating performance was affected by the ambient temperature. As the electric heating power increased, the number of thermal comfort days increased rapidly due to the fact that extremely cold weather occurred less frequently during the heating season. However, higher heating power was required to shift the peak load completely on the coldest day. Based on the results, heating powers of 13 kW and 11.5 kW, respectively, for Strategy A and B were considered sufficient to meet the heating demand of users during the entire heating season.

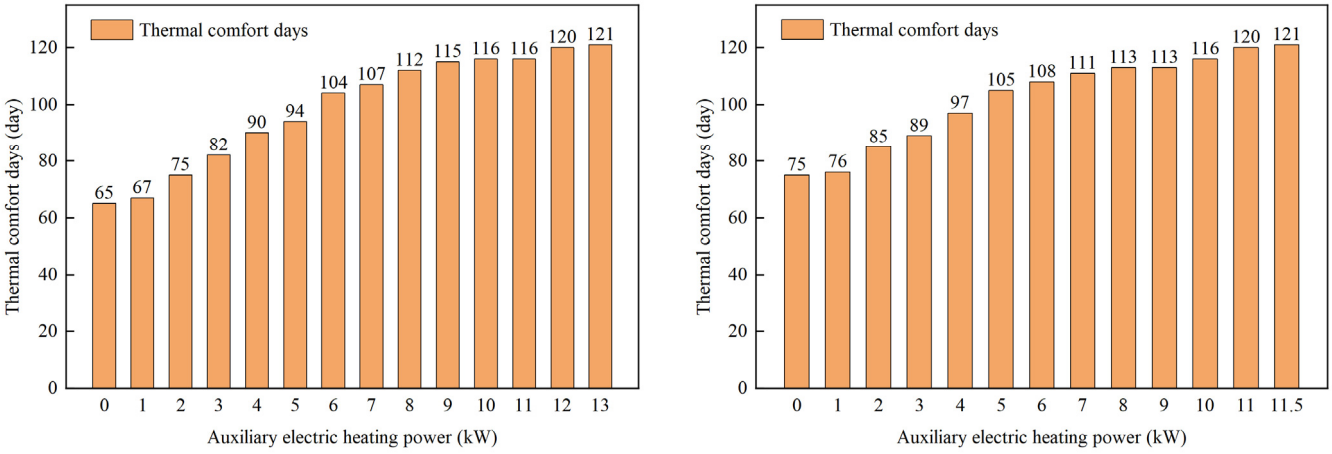

(**a**) Strategy A (**b**) Strategy B

Figure 5. Number of days of thermal comfort during the heating season with different auxiliary electric heating powers. (**a**) Number of thermal comfort days in the heating season corresponding to different heating powers when the system was operated according to Strategy A; (**b**) Number of thermal comfort days in the heating season corresponding to different heating powers when the system was operated according to Strategy B.

Figure 6 illustrates the hourly variation in the water tank temperature and room temperature on a typical day for Strategy A. Here, 6 kW represents a lower auxiliary electric heating power, while 13 kW is the optimized electric heating power for the strategy. During the charging period (2:00–4:30), the water tank temperature rose rapidly, followed by a drop due to standby heat loss from 4:30 to 17:00. During the discharging period (17:00–19:00), the water tank temperature decreased rapidly. Further examination indicates that during the direct heating period of the heat pump (9:00–17:00), the room temperature was maintained at 20 °C. In cases where the auxiliary electric heating power was low, the TES tank failed to reach the temperature set point by the end of the charging period. Therefore, the amount of thermal energy stored during tank charging was not sufficient to offset the heating demand during discharging, leading to a room temperature lower than 20 °C at the end of the discharging period. In contrast, a 13 kW electric heater could ensure the thermal comfort of the occupants during the entire discharging period. Therefore, the use of auxiliary electric heating to raise the storage temperature is necessary for conventional single-stage air source heat pumps to participate in wind curtailment reduction.

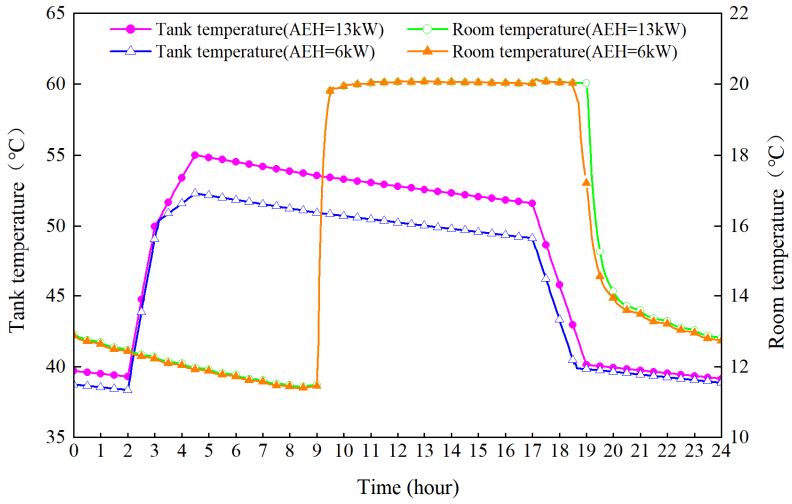

Figure 6. Hourly tank temperature and room temperature in a typical day. (Auxiliary electric heating is abbreviated as AEH).

3.3. Comparison of Operating Strategies

The two operating strategies were compared from various perspectives, including energy consumption, running costs, and wind power utilization. In the simulations, the TES tank size, storage temperature set point, and auxiliary electric heating power were determined according to the optimization results mentioned earlier. In addition, simulations were also conducted for the Base case, in which load-shifting was not considered, and an air source heat pump was used for direct heating during office hours.

Figure 7 illustrates the energy consumption, running costs, and wind utilization for Strategy A, Strategy B, and the Base case in the entire heating season. The energy consumption consisted of wind energy utilization and non-renewable energy consumption. It can be observed that the Base case had the lowest energy consumption, i.e., 8012 kWh. Due to the presence of a standby heat loss in the water tank, both Strategy A and Strategy B needed to store more thermal energy than the actual heat load to achieve the load-shifting purpose. Therefore, their energy consumption was higher than that of the Base case. Specifically, the energy consumption of Strategy A (10,486 kWh) was slightly higher than that of Strategy B (10,340 kWh). This is due to the fact that the charging period of Strategy A ended at 4:30, resulting in a greater standby heat loss compared to Strategy B.

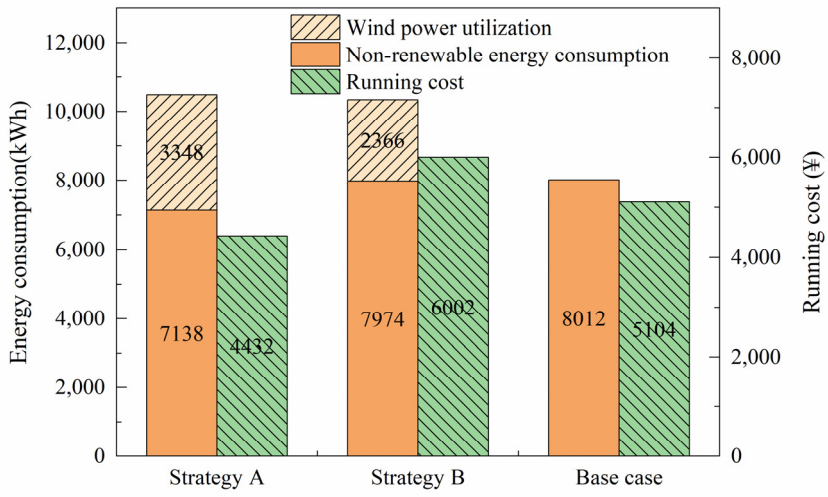

Figure 7. Heating season energy consumption, running costs and wind power utilization for each operating strategy.

The energy consumption of both the heat pump and electric heater, as well as the heat pump COP during the charging period, are compared in Table 4 for the two strategies. Note that even though Strategy B had a charging time later than Strategy A, the ambient temperature was lower at this time. Therefore, Strategy B had a higher heat pump energy consumption due to the decreased efficiency of the heat pump at lower ambient temperatures.

Table 4. Energy consumption and heat pump COP for Strategy A and B in the charging periods.

	Energy Consumption by Heat Pump (kWh)	Energy Consumption by Electric Heater (kWh)	Heat Pump COP during Charging Period
Strategy A	956	2349	2.71
Strategy B	968	2190	2.64

With regards to running costs, although Strategy A consumed more energy than the ones in the Base case and Strategy B, its running costs were the lowest (CNY 4432), which were 13% less than the Base case, as shown in Figure 7. Note that the time-of-use electricity tariff (valley rate: CNY 0.124/kWh, flat rate: CNY 0.62/kWh, peak rate: CNY 1.054/kWh, and sharp peak rate: CNY 1.265/kWh) is used for the three operating strategies. Strategy A was designed to take advantage of both the valley's electricity rates and the high wind power generation, thereby improving its wind power utilization and reducing its running costs. Compared to the Base case (CNY 5104), the charging period for Strategy B corresponded to the flat tariff. However, Strategy B (CNY 6002) obtained higher running costs due to the presence of standby heat loss.

To illustrate the economic feasibility of the proposed system operated with Strategy A, the static payback period for additional system investment was also evaluated. With reference to the local market price, the addition of a storage tank and an electric heater could bring an additional cost of CNY 2900. In addition, it was assumed that the annual maintenance cost of the above equipment was 3% of the additional costs. Based on this, the payback period for the retrofit of the original heat pump system was calculated to be 5 years.

Large-scale wind curtailment mainly occurred between 2:00 and 8:00 (see Figure 1) since early morning was the period of the lowest electricity demand. This paper assumes that the electricity consumed during this time period was generated by wind power. Based on this assumption, the wind power utilization associated with different strategies can be determined. As can be seen in Figure 7, the wind power utilization was highest (3348 kWh) for Strategy A, while the figure was 2366 kWh for Strategy B. Therefore, although both strategies consumed more energy than the Base case, they consumed less non-renewable energy. Strategy A reduced non-renewable energy consumption by 11%.

Accordingly, it can be seen that Strategy A was a more genuine operating strategy for the system because it could maintain thermal comfort, reduce running costs, avoid the grid power demand during peak hours, and allow a higher proportion of wind energy to be integrated into the grid.

4. Conclusions

A single-stage air source heat pump coupled with TES for load shifting and reducing wind power curtailment was proposed in this study. TRNSYS simulations were performed to evaluate the feasibility of the system in a typical building based on actual electricity tariffs, wind power, and meteorological data. The proper system designs, including the tank size and thermal storage temperature, were determined to maximize system performance. The operating strategies of the system were also evaluated from various perspectives, such as energy consumption, running costs, and wind power utilization. The following conclusions were drawn from the research:

1. The size of the water tank and the storage temperature set point determined the system's ability to shift during peak load. For specific applications, a proper combination of the two parameters existed to minimize energy consumption while satisfying the heating demand of users.
2. The use of auxiliary electric heating to raise the storage temperature was necessary for conventional single-stage air source heat pumps to participate in wind curtailment reduction. Different system operating strategies require different capacities for auxiliary heating.
3. By implementing a proper operating strategy, the non-renewable power consumption could be reduced by 11% for the studied building, with a total wind power utilization of 3348 kWh during the heating season while still satisfying the heating demand of users.

The above results confirmed the feasibility of combining a single-stage air source heat pump with thermal storage technology to provide flexible loads to the grid. However, it is worth noting that the energy and economic returns of this technology are affected by conditions such as tariff structures, wind data, and outdoor weather data. Additionally, this paper presented a feasibility study of the proposed system, using a single office building as a case study. Nevertheless, a multi-zone heating system is more representative in practice. Research addressing the above situation will be pursued as future work.

Author Contributions: Conceptualization, J.J.; methodology, Q.R.; software, Q.R. and C.G.; validation, Q.R.; formal analysis, Q.R.; investigation, Q.R.; resources, J.J.; data curation, C.G.; writing—original draft preparation, Q.R.; writing—review and editing, Q.R. and J.J.; visualization, J.J.; supervision, C.G.; project administration, J.J.; funding acquisition, J.J. All authors have read and agreed to the published version of the manuscript.

Funding: This study is funded by the National Natural Science Foundation of China (No. 51808372), Science and Technology Cooperation and Exchange Project of Shanxi Province (202104041101025), and Shanxi Provincial Science and Technology Major Special Program (202101060301015).

Data Availability Statement: The data are not publicly available due to research confidentiality requirements.

Conflicts of Interest: Author Chuang Gao was employed by the company CSSC International Engineering Co., Ltd. The remaining authors declare that the research was conducted in the absence of any commercial or financial relationships that could be construed as a potential conflict of interest.

Nomenclature

m	fluid flow rate (kg/s)
C	fluid heat transfer coefficient (kJ/kg·K)
T	temperature (°C)
Q	heat flow rate (kW)
V	volume of tank (m^3)
H	height of the tank (m)
U	heat loss coefficient ($W/(m^2 \cdot K)$)
L	circumference of tank (m)
Subscript	
i	the ith node
fl	fluid
heat	heat source side
load	load side
aux	auxiliary electric heater
loss	loss of heat
bot	bottom of the tank
top	top of the tank
N	number of tank layers
t	tank
env	environment

References

1. Hewitt, J.N. Heat pumps and energy storage—The challenges of implementation. *Appl. Energy* **2012**, *89*, 37–44. [CrossRef]
2. Hedegaard, K.; Mathiesen, B.V.; Lund, H.; Heiselberg, P. Wind power integration using individual heat pumps—Analysis of different heat storage options. *Energy* **2012**, *47*, 284–293. [CrossRef]
3. Bloess, A.; Schill, W.; Zerrahn, A. Power-to-heat for renewable energy integration: A review of technologies, modeling approaches, and flexibility potentials. *Appl. Energy* **2018**, *212*, 1611–1626. [CrossRef]
4. Wu, P.; Wang, Z.; Li, X.; Xu, Z.; Yang, Y.; Yang, Q. Energy-saving analysis of air source heat pump integrated with a water storage tank for heating applications. *Build. Environ.* **2020**, *180*, 107029. [CrossRef]
5. Ermel, C.; Bianchim, V.; Cardoso, A.P.; Schneider, P.S. Thermal storage integrated into air-source heat pumps to leverage building electrification: A systematic literature review. *Appl. Therm. Eng.* **2022**, *215*, 118975. [CrossRef]
6. Le, K.X.; Huang, M.J.; Wilson, C.; Shah, N.N.; Hewitt, N.J. Tariff-based load shifting for domestic cascade heat pump with enhanced system energy efficiency and reduced wind power curtailment. *Appl. Energy* **2020**, *257*, 113976. [CrossRef]
7. Wang, Z.; Zhang, Y.; Wang, F.; Li, G.; Xu, K. Performance Optimization and Economic Evaluation of CO_2 Heat Pump Heating System Coupled with Thermal Energy Storage. *Sustainability.* **2021**, *13*, 13683. [CrossRef]
8. Zhang, D.; Fang, C.; Shen, C.; Chen, S.; Li, H.; Qin, X.; Liu, H.; Wu, X. 4E analysis and multi-objective optimization of compression/ejection transcritical CO_2 heat pump with latent thermal heat storage. *J. Energy Storage* **2023**, *72*, 108475. [CrossRef]
9. Vivian, J.; Prataviera, E.; Cunsolo, F.; Pau, M. Demand Side Management of a pool of air source heat pumps for space heating and domestic hot water production in a residential district. *Energy Convers. Manag.* **2020**, *225*, 113457. [CrossRef]
10. Fitzpatrick, P.; D'Ettorre, F.; Rosa, D.M.; Yadack, M.; Eicker, U.; Finn, D.P. Influence of electricity prices on energy flexibility of integrated hybrid heat pump and thermal storage systems in a residential building. *Energy Build.* **2020**, *223*, 110142. [CrossRef]
11. Maarten, E.; Alice, M.; Alessia, A. Design energy flexibility characterisation of a heat pump and thermal energy storage in a Comfort and Climate Box. *Appl. Therm. Eng.* **2022**, *216*, 119154.
12. Badescu, V. Model of a thermal energy storage device integrated into a solar assisted heat pump system for space heating. *Energy Convers. Manag.* **2003**, *44*, 1589–1604. [CrossRef]
13. Lyu, W.; Wang, Z.; Li, X.; Deng, G.; Xu, Z.; Li, H.; Yang, Y.; Zhan, B.; Zhao, M. Influence of the Water tank size and air source heat pump size on the energy saving potential of the energy storage heating system. *J. Energy Storage* **2022**, *55*, 105542. [CrossRef]
14. Miara, M.; Günther, D.; Leitner, Z.L.; Wapler, J. Simulation of an Air-to-Water Heat Pump System to Evaluate the Impact of Demand-Side-Management Measures on Efficiency and Load-Shifting Potential. *Energy Technol.* **2014**, *2*, 90–99. [CrossRef]
15. Arteconi, A.; Hewitt, N.; Polonara, F. Domestic demand-side management (DSM): Role of heat pumps and thermal energy storage (TES) systems. *Appl. Therm. Eng.* **2013**, *51*, 155–165. [CrossRef]
16. Kelly, N.J.; Tuohy, P.G.; Hawkes, A.D. Performance assessment of tariff-based air source heat pump load shifting in a UK detached dwelling featuring phase change-enhanced buffering. *Appl. Therm. Eng.* **2014**, *71*, 809–820. [CrossRef]
17. Wang, Y.; Qiu, J.; Tao, Y. Robust energy systems scheduling considering uncertainties and demand side emission impacts. *Energy* **2022**, *239*, 122317. [CrossRef]
18. Li, Z.; Wu, L.; Xu, Y.; Zheng, X. Stochastic-Weighted Robust Optimization Based Bilayer Operation of a Multi-Energy Building Microgrid Considering Practical Thermal Loads and Battery Degradation. *IEEE Trans. Sustain. Energy* **2022**, *13*, 668–682. [CrossRef]
19. Ding, B.; Li, Z.; Li, Z.; Xue, Y.; Chang, X.; Su, J.; Jin, X.; Sun, H. A CCP-based distributed cooperative operation strategy for multi-agent energy systems integrated with wind, solar, and buildings. *Appl. Energy* **2024**, *365*, 123275. [CrossRef]
20. Hao, J.; Gou, X.; Wang, S.; Chen, Q.; Gao, K. Dynamic Modeling and Flexibility Analysis of an Integrated Electrical and Thermal Energy System with the Heat Pump–Thermal Storage. *Front. Energy Res.* **2022**, *10*, 817503. [CrossRef]
21. Fischer, D.; Madani, H. On heat pumps in smart grids: A review. *Renew. Sustain. Energy Rev.* **2017**, *70*, 342–357. [CrossRef]
22. Salpakari, J.; Lund, P. Optimal and rule-based control strategies for energy flexibility in buildings with PV. *Appl Energy* **2016**, *161*, 425–436. [CrossRef]
23. Le, H.; Li, H.; Jiang, Y. Realization of Substituting Coal with Electricity and Enhancing the Efficiency of Electricity Allocation by Using Air Source Heat Pump. *Energy China* **2016**, *38*, 9–15.
24. The People's Government of Hebei Province: Hebei Provincial Development and Reform Commission Notice on Further Improving the Time-Sharing Electricity Pricing Policy for Industrial, Commercial and Other Users in Hebei South Network. Available online: https://hbdrc.hebei.gov.cn/xxgk_2232/zc/wzcwj/202309/t20230907_92155.html (accessed on 28 October 2022).